MODELING AND DATA ANALYSIS OF A PALLADIUM MEMBRANE REACTOR FOR TRITIATED IMPURITIES CLEANUP

Stephen A. Birdsell and R. Scott Willms
Mail Stop C-348
Los Alamos National Laboratory
Los Alamos, NM 87545
505-667-1710

ABSTRACT

A model was developed to explore the use of a palladium membrane reactor for fusion fuel processing. The model was benchmarked to tritium-containing experiments that simulated the expected plasma exhaust of the International Thermonuclear Experimental Reactor. This modeling effort has greatly improved our understanding of the processes occuring in the reactor.

I. INTRODUCTION

A palladium membrane reactor (PMR) is under consideration for the tritium plant for the International Thermonuclear Experimental Reactor (ITER). The ITER reactor exhaust will contain tritiated impurities such as water and methane. Tritium will need to be recovered from these impurities for environmental and economic reasons. For this purpose a promising device, called the PMR, has been proposed. The PMR is a combined permeator and catalytic reactor. Nickel catalysts are used to foster reactions such as water-gas shift, $H_2O + CO \rightarrow H_2 + CO_2$, and methane steam reforming, $CH_4 + H_2O \rightarrow 3H_2 + CO$. Due to thermodynamic limitations these reactions only proceed to partial completion. Thus, a Pd/Ag membrane, which is exclusively permeable to hydrogen isotopes, is incorporated into the reactor. By maintaining a vacuum on the permeate side of the membrane, product hydrogen isotopes are removed, enabling the reactions to proceed to completion.

Others have used membrane reactors to reform methane to conversions beyond normal equilibrium to demonstrate this technology for industrial applications. Uemiya et al.[1] used a Pd membrane on Vycor glass with Ni catalyst. Tsotsis et al.[2] used a commercially available microporous alumina membrane with Ni catalyst. Shu et al.[3] used a Pd/Ag membrane with Ni catalyst, which is the most similar to the reactor in this study. Although these reactors produced conversions greater than the normal equilibrium limit, they did not remove essentially all of the hydrogen as will be required in fusion fuel processing. Good conversions in an industrial application would be 50-90%, while we are interested in achieving over 99% conversion.

A model has been developed to study the complex interactions in a PMR so that the optimal design can be determined. The model accounts for the coupled effects of transport-limited permeation of hydrogen isotopes and chemical reactions. The permeation model is an extension of previous models that include the effects of temperature, wall thickness, reaction-side pressure, and permeate-side pressure. Reaction rates for methane steam reforming and the water-gas shift reaction are incorporated into the model along with the respective reverse reactions.

The reverse reactions become important as equilibrium is approached. The injected gas mixture is initially far from equilibrium and only the forward reactions are important. As hydrogen is removed from the reacting stream, equilibrium concentrations shift in favor of further impurities conversion. Nevertheless, the methane and water concentrations eventually approach the equilibrium values and the reverse reactions become important.

The model is compared to PMR experimental data and used to investigate the concentration and pressure profiles in the reactor. Due to the interactions of permeation and reaction, complex profiles can be produced in a PMR. For example, in the data presented in this paper, the water concentration often increases after the inlet to the PMR, forms a maximum value, and then decreases to the low values expected with a PMR. Detailed information like this is useful for the design and optimization of PMRs for the ITER tritium plant.

Table 1. Experimental conditions and results from Willms et al.[4]

Parameter	Test 1	Test 3
Nominal T (°C)	505	572
P (atm)	1.19	1.20
Input		
Inert Feed (std. cm^3/min)	22.0	12.8
CQ_4 Feed (std. cm^3/min)	20.0	13.1
Q_2O Feed (std. cm^3/min)	25.2	17.0
Q_2 Feed (std. cm^3/min)	5.2	3.0
Output		
Inert (mole %)	61.5	61.2
CQ_4 (mole %)	0.195	0.210
Q_2O (mole %)	0.310	0.058
Q_2 (mole %)	0.133	0.110
CO (mole %)	2.45	2.98
CO_2 (mole %)	35.7	34.9
Retentate Flow (std. cm^3/min)	34.2	25.5
Permeate Pressure (atm)	5.26×10^{-4}	6.58×10^{-4}
Permeate Flow (std. cm^3/min)	69.4	48.0
DF	250	307

II. EXPERIMENT DESCRIPTION

Willms et al.[4] gives a detailed description of the experiments and experimental results, therefore, only a synopsis will be given here. Experiments were conducted with an inlet mixture that the ITER Tritium Plant team is considering as the design mixture for the exhaust of the ITER reactor. The Pd/Ag tube in the PMR was 52 cm in length and had an OD of 0.50 cm. This tube was placed inside a 2.21 cm ID tube and the annulus was filled with Ni/Al_2O_3 catalyst. Feed was injected into one end of the annulus and retentate flowed out the other end. Permeate was removed from the inside of the Pd/Ag tube with a vacuum pumping system. Table 1 shows the inlet and outlet conditions for the two experiments analyzed with the PMR model in this paper. Test 1 was the initial tritium experiment and 2.2 % of all hydrogen isotopes (Q_2, Q_2O, and CQ_4) were tritium the balance hydrogen. In Test 3, 43.3 % of the hydrogen isotopes were tritium and the balance was hydrogen.

III. MODEL DESCRIPTION

A model was developed to investigate the performance of PMRs operating at ITER fuel cleanup conditions. Xu and Froment[5] have studied the methane steam reforming process extensively and have determined three dominant reactions:

$$CH_4 + H_2O \leftrightarrow CO + 3H_2 \quad (1)$$

$$CO + H_2O \leftrightarrow CO_2 + H_2 \quad (2)$$

$$CH_4 + 2H_2O \leftrightarrow CO_2 + 4H_2 \quad (3)$$

They determined intrinsic rates for these reactions in the form of Langmuir-Hinshelwood kinetics:

$$R_1 = \frac{k_1}{P_{H_2}^{2.5} Den^2}\left(P_{CH_4} P_{H_2O} - \frac{P_{H_2}^3 P_{CO}}{K_{eq,1}}\right) \quad (4)$$

$$R_2 = \frac{k_2}{P_{H_2} Den^2}\left(P_{CO}\, P_{H_2O} - \frac{P_{H_2} P_{CO_2}}{K_{eq,3}}\right) \quad (5)$$

$$R_3 = \frac{k_3}{P_{H_2}^{3.5} Den^2}\left(P_{CH_4} P_{H_2O}^2 - \frac{P_{H_2}^4 P_{CO_2}}{K_{eq,3}}\right) \quad (6)$$

where

Table 2. Arrhenius parameters for the reaction rate expressions (Xu and Froment, 1989).

Rate or Adsorption constant	A_i	E_i/R (K^{-1})
k_1	1.17×10^{12} (mol-atm$^{1/2}$/g-s)	28900
k_2	5.50×10^{2} (mol/g-s-atm)	8070
k_3	2.82×10^{11} (mol-atm$^{1/2}$/g-s)	29300
K_{CO}	8.34×10^{-5} (atm^{-1})	-8500
K_{H2}	6.20×10^{-9} (atm^{-1})	-9970
K_{H2O}	1.77×10^{5}	10700
K_{CH4}	6.74×10^{-4} (atm^{-1})	-4600

$$Den = 1 + K_{CO}P_{CO} + K_{H_2}P_{H_2} + K_{CH_4}P_{CH_4} + K_{H_2O}P_{H_2O} / P_{H_2}$$

and the preexponential factors and activation energies for the reaction rate constants (k_1, k_2, and k_3) and adsorption constants (K_{CO}, K_{H2}, K_{H2O}, and K_{CH4}) are shown in Table 2. $K_{eq,1}$, $K_{eq,2}$, and $K_{eq,3}$ are the equilibrium constants for eqns. 1-3. The model assumes that the flow is one dimensional, steady-state and isothermal[a]. Continuity equations for the retentate are:

$$dF_{CO} = W_{cat}(R_1 - R_2)dz \quad (7)$$

$$dF_{H_2,ret} = \left[W_{cat}\left(3R_1 + R_2 + 4R_3\right) - R_{perm}\right]dz \quad (8)$$

$$dF_{CH_4} = -W_{cat}\left(R_1 + R_3\right)dz \quad (9)$$

$$dF_{CO_2} = W_{cat}(R_2 + R_3)dz \quad (10)$$

$$dF_{H_2O} = -W_{cat}(R_1 + R_2 + 2R_3)dz \quad (11)$$

In the above model, H represents both hydrogen and tritium. The permeation model accounts for the different rates of the two hydrogen isotopes[6]:

$$dF_{Q_2,perm} = R_{perm}dz \quad (12)$$

$$R_{perm} = K_{perm,i}\left(\sqrt{P_{Q_{2,ret}}} - \sqrt{P_{Q_{2,perm}}}\right) \quad (13)$$

$$K_{perm,i} = \frac{2\pi A_i}{\ln\left(\frac{r_{in}}{r_{out}}\right)}\exp\left(\frac{-E_i}{T}\right) \quad (14)$$

where $K_{perm,i}$ is a weighted average of the pure hydrogen permeation factor and the pure tritium permeation factor. The Arrhenius parameters for hydrogen and tritium permeation are[7]:

$$A_{H_2} = 1.23\times10^{-7}\left(\frac{mol}{cm-s-atm^{0.5}}\right) \quad (15)$$

$$E_{H_2} = 689K^{-1} \quad (16)$$

$$A_{T_2} = 6.34\times10^{-8}\left(\frac{mol}{cm-s-atm^{0.5}}\right) \quad (17)$$

$$E_{T_2} = 740K^{-1} \quad (18)$$

Film theory was used to calculate the effect of diffusion on the permeation rate

$$R_{perm} = \frac{2\pi r k_m}{RT}\left(P_{Q_{2,wall}} - P_{Q_{2,perm}}\right) \quad (19)$$

where r is the outer radius of the membrane tube and the mass transfer coefficient, k_m, calculated from the Sherwood number correlation[8].

$$Sh = k_m D\left(3.66^3 + 1.61^3\,\mathrm{Re}\,Sc\frac{D}{L}\right)^{1/3} / D_{Q_2-mix} \quad (20)$$

Physical properties were calculated locally with the Chemkin Thermodynamic Data Base code for determining properties of gas mixtures[9]. The diameter used in the Re calculation is the particle diameter

[a] Pressure drop is calculated with the Ergun equation in the computer code but this is not presented here since the data analyzed in this paper are essentially isobaric

$$D_p = \sqrt{2r_p L_p + 2r_p^2} \quad (21)$$

based on the length and radius of the catalyst pellets. The diameter used in the Sh calculation is the diameter of the retentate tube, which assumes that hydrogen diffusion within the retentate annulus is not effected by the presence of the catalyst.

The above equations were solved with a fourth order Runge-Kutta method.

Equilibrium between the reactions in eqns. 1-3 is accounted for in the reaction rate model (eqns. 4-6). However, initial calculations showed that the model and data did not agree using this estimate of the equilibrium. Therefore, equilibrium was calculated for our data using the computer code Solgas[10]. Solgas calculations indicated that carbon was depositing as coke in the reactor and this significantly effected the gas phase equilibrium. These calculations were in good agreement with the PMR data. Therefore, coking was accounted for by incorporating Solgas results into the PMR model. Figure 1 shows the results of Solgas calculations based on the inlet conditions for Test 1. Shown is the fraction of total carbon fed which deposits as coke versus the fraction of the total hydrogen isotopes fed which have been removed by permeation. This relationship can be incorporated into the PMR model without introducing significant error because our data are isothermal and isobaric. The carbon balance was adjusted according to Figure 1 via the methane decomposition reaction:

$$CH_4 \leftrightarrow C(s) + 2H_2 \quad (22)$$

This method of estimating coke formation assumes that the methane decomposition reaction moves to equilibrium instantaneously.

Reactions other than the methane decomposition could be the route to carbon formation. In this model, it does not matter what reaction we use to incorporate the quantity of coke formed. For expample, accounting for coke formation via the Bourdart reaction

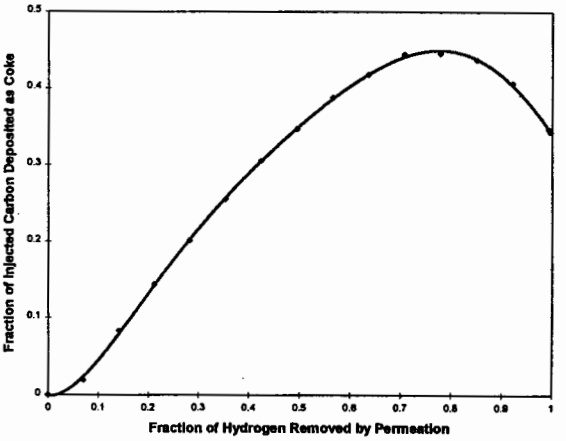

Figure 1. Equilibrium carbon deposition as a function of hydrogen removal for Test 1 (calculated with Solgas)[10].

$$2CO \leftrightarrow C(s) + CO_2 \quad (23)$$

yields the same results as using the methane decomposition reaction. This is because the carbon-formation model is only a change in the gas-phase carbon inventory. Once the carbon inventory is changed, the other equilibrium reactions in the model (eqns. 1-6) adjust properly.

IV. MODEL RESULTS

Table 3 shows the outlet composition for the Test 1 data compared to the PMR rate model and the Solgas equilibrium model. The rate and equilibrium models agree well, confirming that the hybrid equilibrium model (combination of reaction rates from Xu and Froment[5] and Solgas[10]) in the PMR model is appropriate. It is evident that the coke formation is in equilibrium from the comparison of the experimental and predicted quantity of deposited carbon. Also, the data are within 20% of equilibrium for the water-gas shift reaction (eqn. 2). However, the methane reforming reaction (eqn. 1) is far from equilibrium.

Figure 2 shows the decontamination factor (inlet total tritium flow rate divided by the outlet total tritium flow rate) calculated with the model for Test 1. The model

Table 3. Outlet composition (mole %) from data and calculated from the PMR rate model and the Solgas equilibrium model for Test 1 (504 C, 1.19 atm, outlet decontamination factor=250).

	CO	CO_2	H_2	Inert (He&Ar)	H_2O	CH_4	% Carbon deposited
Data	**2.45**	**35.7**	**0.133**	**61.5**	**.31**	**.195**	**34.4**
PMR Rate Model	**3.18**	**33.7**	**0.259**	**62.3**	**0.573**	**1.18×10^{-3}**	**34.3**
Solgas Equilibrium Model	**3.57**	**33.6**	**0.274**	**62.1**	**0.517**	**1.92×10^{-3}**	**34.3**

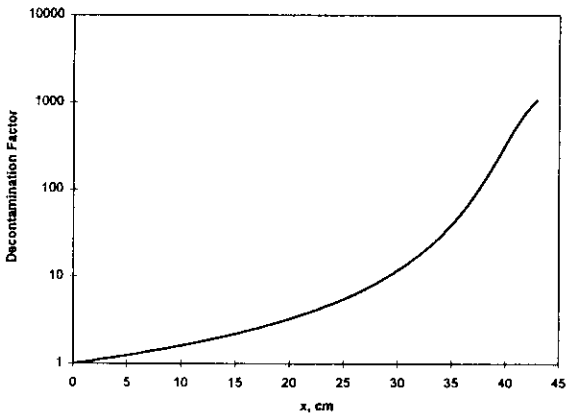

Figure 2. Model results for the decontamination factor for Test 1.

predicts that the experimental decontamination factor of 250 is achieved at 40 cm from the entrance to the reactor. The model results shown in Table 3 are given at this point. Indeed, the best decontamination factor that can be achieved is when the retentate is in thermodynamic equilibrium and the hydrogen partial pressure in the retentate is in equilibrium with the permeate pressure. This equilibrium decontamination factor is 1125 for Test 1 and is predicted by the model to be achieved at approximately 50 cm from the entrance to the reactor.

Comparison of model and experimental decontamination factor for Test 3 is similar. In this case, the experimental decontamination factor of 360 was predicted to occur at 44 cm from the inlet to the reactor. Several possible explanations exist for the discrepancy between the theoretical lengths calculated for Tests 1 and 3 and the experimental lengths. First, reaction rates could be in error. The reaction rates of Xu and Froment[5] were modified for this model, but more importantly, those rates were determined from data at industrial operating conditions which are at much higher H_2O concentrations (to prevent coking) and much higher H_2 concentrations (H_2 is not removed with permeators in industrial applications). Second, experimental error could cause the discrepancy. As mentioned in Willms et al., some problems were encountered measuring the temperature in the reactor during the experiments. It is plausible that the tests were run at a temperatures somewhat below the reported values. This explanation is weakened by the above discussion that indicates the data are in equilibrium (with the exception of the stable methane molecule) at the reported experiment temperature. Finally, it is possible that our catalyst was deactivated by coke formation on active sites.

Figure 3 shows the calculated flow profiles of carbon-containing species in the reactor for Test 1. In this plot, F_C is the fraction of the injected carbon that has been deposited as coke. Figure 4 shows the flow profiles of hydrogen-containing species. Figure 5 shows the composition profiles for methane and water. The model predicts that, close to the entrance of the reactor, water reacts slowly and is actually concentrated due to the high permeation rate. Finally, Figure 6 shows the hydrogen gradient between the bulk gas and the gas next to the membrane. It can be seen that the diffusion limitation caused by the hydrogen flux through the membrane is significant but not dramatic.

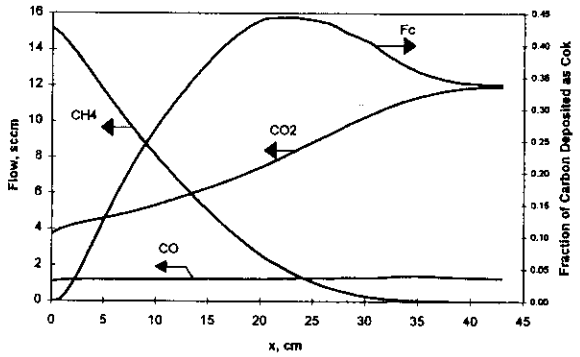

Figure 3. Model predictions of carbon-containing species for Test 1.

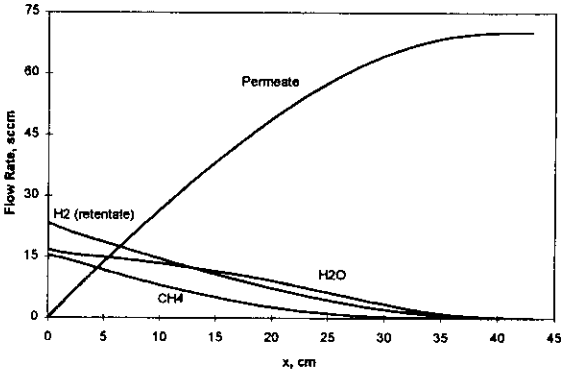

Figure 4. Model predictions of hydrogen-containing species for Test 1.

Table 4. Outlet composition (mole %) from data and calculated from the PMR rate model and the Solgas equilibrium model for Test 3 (572 C, 1.20 atm, and outlet decontamination factor=307)

	CO	CO_2	H_2	Inert (He&Ar)	H_2O	CH_4	% Carbon deposited
Data	2.98	34.9	0.11	61.2	0.058	0.21	36.3
PMR Rate Model, no carbon uptake	3.60	36.9	0.141	58.9	0.481	1.66×10^{-5}	32.4
PMR Rate Model	12.7	30.7	0.330	56.0	0.266	1.36×10^{-3}	27.0
Solgas Equilibrium Model	10.2	32.4	0.301	56.7	0.300	7.74×10^{-4}	26.5

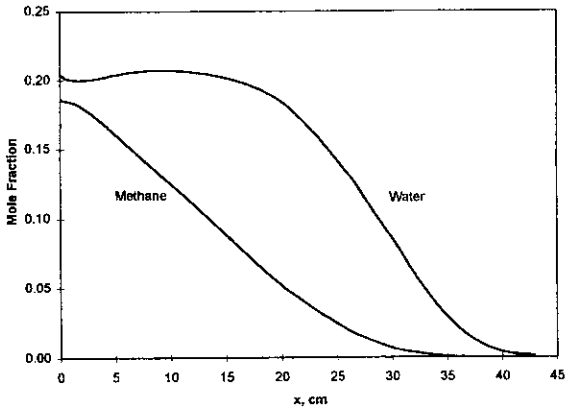

Figure 5. Model predictions of methane and water fractions for Test 1.

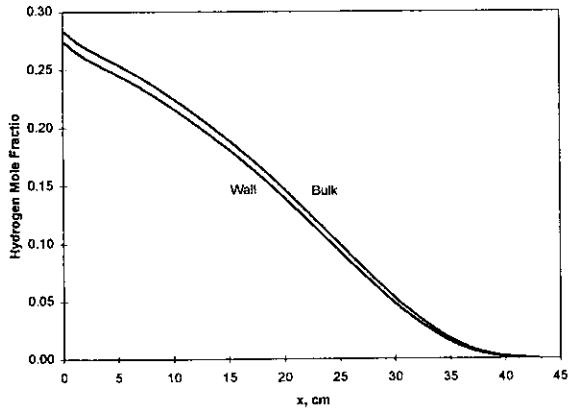

Figure 6. Model predictions for hydrogen gradient across a thin film at the membrane surface for Test 1.

Table 4 shows the results of Test 3, which resulted in a decontamination factor of 307 at a temperature of 572 C. The table shows two PMR model results. The first result does not allow carbon to be transferred from solid coke into the gas phase. The second result allows carbon uptake to occur. Comparison of F_C in Figure 7 to that in Figure 3 demonstrates the difference between these 2 cases. The case with no carbon uptake allowed fits the data of Test 3 much better than the case in which carbon uptake is allowed. Therefore, it is postulated that no coke was available for uptake in the latter part of the reactor during Test 3. For Test 1, however, there may have been carbon leftover from previous startup actibities.

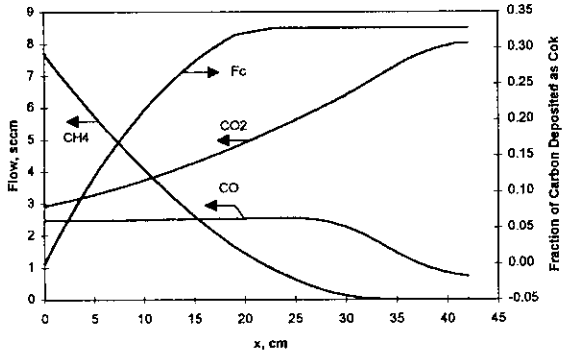

Figure 7. Model prediction of carbon-containing species for Test 3.

By way of comparison, Table 5 shows the Test 3 PMR rate model and the Solgas equilibrium model results when the models were constrained to not allow carbon formation. There is a dramatic difference between the predicted and measured outlet concentrations when carbon deposition is not accounted for. These errors were eliminated when the mechanism for carbon deposition (eqn. 19) was incorporated into the code as shown on Table 4.

Table 5. Same as Table 4, except PMR rate model and Solgas equilibrium model do not allow carbon deposition.

	CO	CO_2	H_2	Inert (He&Ar)	H_2O	CH_4	% Carbon deposited
Data	**2.98**	**34.9**	**0.11**	**61.2**	**0.058**	**0.21**	**36.3**
PMR Rate Model (no carbon)	**35.2**	**15.0**	**0.404**	**49.2**	**0.0574**	**0.0324**	-
Solgas Equilibrium Model (no carbon)	**35.4**	**15.0**	**$3.99x10^{-6}$**	**49.2**	**$5.35x10^{-6}$**	**$3.50x10^{-6}$**	-

V. CONCLUSIONS

A PMR model has been developed and compared to tritium-containing experiments relevant to ITER. The model uses intrinsic kinetics for methane steam reforming. The kinetics are adapted to ITER conditions by adding carbon deposition via the methane decomposition reaction. The model shows that it is possible for regions of coking and decoking to exist within a PMR. These effects do not result in lower decontamination factors.

This model has led to a better understanding of PMRs operating at ITER conditions and will be useful in the design and operation of future PMR experiments. Benchmarking of the model to PMR data elucidated the need to incorporate a coking mechanism into the model. It is intended that this model will be developed into a robust model that includes coking reaction rates and fully-coupled gas-coke equilibrium.

ACKNOWLEDGMENTS

This research was sponsored by the United States Department of Energy, Office of Fusion Energy. The model development and computer support from Michael A. Inbody (Los Alamos National Laboratory) was greatly appreciated.

NOMENCLATURE

A	Preexponential Factor
D	Diameter (cm)
$D_{H2\text{-}mix}$	Diffusivity of H_2 in the local gas mixture (cm^2/s)
DF	Decontamination Factor, inlet tritium flow rate divided by the outlet tritium flow rate
E	Activation Energy (K^{-1})
F_i	Molar Rate (mol/s)
k_i	Reaction Rate Constant for reactions i=1, 2, and 3 (see Table 1 for units)
k_m	Mass Transfer Coefficient (cm/s)
K_i	Adsorption Constant for species i= CO, H_2, H_2O, and CH_4 (see Table 1 for units)
$K_{eq,i}$	Equilibrium Constants for reactions i=1, 2, and 3.
$K_{perm,i}$	Permeation Factor for H_2 and T_2
L	Length (cm)
P	Pressure (atm)
Q_2	Hydrogen Isotopes
r	Radius (cm)
Re	Reynold's Number
R_i	Reaction Rate (mol/g-s) or Permeation Rate (mol/cm-s)
R	Universal Gas Constant
Sc	Schmidt Number
T	Temperature (K)
Sh	Sherwood Number
W_{cat}	Linear density of catalyst (g/cm)
z	Axial Length of Reactor (cm)

SUBSCRIPTS

p	Catalyst pellet
perm	Permeation
ret	Retentate
wall	At the membrane wall

REFERENCES

1. Uemiya, S., Sato, N., Ando, H., Matsuda, T. and E. Kikuchi, "Steam Reforming Of Methane In A Hydrogen-Permeable Membrane Reactor," *Applied Catalysis*, **67** (1991), 223-230.

2. Tsotsis, T. T., Champagnie, A. M., Vasileiadis, S. P., Ziaka, Z. D. and R. G. Minet, "The Enhancement Of Reaction Yield Through The Use Of High Temperature Membrane Reactors," *Separation Science and Technology*, **28** (1-3), (1993), 397-422.

3. Shu, J., Grandjean, B. P. A. and S. Kaliaguine, "Methane Steam Reforming In Asymmetric Pd- And Pd-Ag/Porous SS Membrane Reactors," *Applied Catalysis*, **119** (1994) 305-325.

4. Willms, R. S., Birdsell, S. A. and R. C. Willhelm, "Recent Palladium Membrane Reactor Development At The Tritium Systems Test Assembly," To appear in the Proceedings of the *Fifth Topical Meeting on Tritium Technology In Fission, Fusion And Isotopic Applications*, Lake Maggiore, Italy, May 28-June3, 1995.

5. Xu, J. and G. F. Froment, "Methane Steam Reforming, Methanation and Water-Gas Shift: I. Intrinsic Kinetics," *AIChE Journal*, Jan. 1989, Vol. **35**, No. **1**, 88-96.

6. Ackerman, F. J. and G. J. Koskinas, "A Model for Predicting the Permeation of Hydrogen-Deuterium-Inert Gas Mixtures through Palladium Tubes," *Ind. Eng. Chem. Fundam.*, 1972, Vol. **11**, No. 3, 332-338.

7. Yoshida, H., Konishi, S. and Naruse Y., "Preliminary Design of a Fusion Reactor Fuel Cleanup System by the Palladium-Alloy Membrane Method," *Nuclear Technology/Fusion*, May 1983, Vol. **3**, 471-484.

8. Rautenbach, R. and R. Albrecht, *Membrane Processes*, John Wiley & Sons, New York, 1989, p. 82.

9. Kee, R. J., Rupley, F. M. and J. A. Miller, "The Chemkin Thermodynamic Data Base," Sandia National Laboratories Report, SAND87-8215B (1990).

10. Besmann, T. "Solgasmix-PV for the PC," Oak Ridge National Laboratory Report, Oak Ridge National Laboratory, Oak Ridge, TN, Oct 24, 1989.